

# Surface Functionalization of TiO<sub>2</sub> with Plant Extracts and their Combined Antimicrobial Activities Against *E. faecalis* and *E. Coli*

Archana Maurya<sup>1,\*</sup>, Pratima Chauhan<sup>1</sup>, Amita Mishra<sup>2</sup> and Abhay K. Pandey<sup>2</sup>

<sup>1</sup>UGC Center of Advanced Studies, Department of Physics, University of Allahabad, Allahabad-211002, India

<sup>2</sup>Department of Biochemistry, University of Allahabad, Allahabad-211002, India

**Abstract:** The aim of this study is to enhance the antibacterial activity of TiO<sub>2</sub> by pure plant extracts of *Bauhinia variegata* and *Tinospora cordifolia* by making a composite of plant extract and TiO<sub>2</sub>. Plant extracts, TiO<sub>2</sub> and plant extracts/TiO<sub>2</sub> composites were investigated against two bacterial strain *Enterococcus faecalis* and *Escherichia coli*. X-ray diffraction investigations have confirmed the presence of TiO<sub>2</sub> nanoparticles in the plant extract/TiO<sub>2</sub> nanocomposites. UV-visible investigations have shown an enhanced photocatalytic activity of plant extract/TiO<sub>2</sub> nanocomposites compared to that of pure TiO<sub>2</sub> and pure plant extract. Plant extract/TiO<sub>2</sub> nanocomposites have shown various level of antibacterial activity on different test microorganisms. The highest antibacterial potentiality expressed in terms of zone of inhibition (ZOI) in mm was exhibited by the aqueous extract of *Bauhinia variegata* /TiO<sub>2</sub> (45 mm against *Enterococcus faecalis* and 30 mm against *Escherichia coli*) and benzene extract of *Tinospora cordifolia* /TiO<sub>2</sub> (26 mm) nanocomposites. This is the first study on these types of bio-nano composite materials and it serves as basis for further research on these types of composite materials as a potent antibacterial agent.

**Keywords:** Titanium dioxide, antimicrobial activity, *Enterococcus faecalis*, *Escherichia coli*.

## 1. INTRODUCTION

Microorganisms are responsible for millions of deaths and many millions of cases of disease and disability each year. The ability to control or destroy microorganisms is therefore of enormous importance to many organizations and industries e.g. healthcare, food and drink, water treatment and military. *Enterococcus faecalis* (*E. faecalis*) is a genus of lactic acid bacteria of the phylum Firmicutes. Enterococci are Gram-positive cocci that often occur in pairs or short chains. They are found in the intestine of nearly all animals, from cockroaches to humans. Important clinical infections caused by *Enterococcus* include urinary tract infections, bacteremia, bacterial endocarditis, diverticulitis, and meningitis [1, 2]. Enterococci are usually considered strict fermenters because they lack a Krebs's cycle and respiratory chain [3]. *Escherichia coli* (*E. coli*) is a Gram-negative bacteria that is well known for its toxicity to humans, being the cause of afflictions ranging from inflammations and peritonitis to food poisoning and urinary infections [4]. This toxicity has led to the development of many strategies to disinfect various media of these organisms [5].

Recently, great efforts have been made to develop nanostructured composite materials where bioactive compounds are embedded within an inorganic nanostructured matrix [6]. Nanocomposites may combine biopolymers that mimic the organic

component of the extracellular matrix of bone (e.g., collagen) and bioactive nanoceramics to induce biomineralization [7]. It has already been recognized that structural aspects can also have profound influences on the cell function, fate and tissue formation [8]. Surface modification of biomaterials with the intent to improve not only biocompatibility but also target cell and/or tissue response has been extensively studied. Biomaterials with nanoscale organizations can be used as controlled-release reservoirs for drug delivery and as a promising tool to support cell therapy. The nanoscaffolds can be synthesized with controlled composition, shape, size, morphology and their surface properties can be manipulated to increase solubility, immunocompatibility, and cellular uptake.

TiO<sub>2</sub> is one of the most widely used material owing to its many applications in the field of photocatalysis, gas and humidity sensors, water treatment, self-cleaning, solar cells, photo electrochemical cells, protective coatings on optical elements and bio-analytical chemistry [9-13]. It is also widely employed as a pigment to provide whiteness and opacity to products such as paints, coatings, plastics, papers, inks, sunscreen, foods, medicines as well as most toothpastes [14-20]. The TiO<sub>2</sub> photocatalysts have been investigated extensively for the killing or growth inhibition of bacteria, with the benefits of physicochemical stability, nontoxicity, bio-compatibility, and low-cost [21-23]. Being strong oxidant, the reactive oxygen species generated by the TiO<sub>2</sub> photocatalytic reactions cause various damages to microorganisms ensuring their rapid inactivation. Matsunaga *et al.* [24]

\*Address corresponding to this author at the UGC Center of Advanced Studies, Department of Physics, University of Allahabad, Allahabad-211002, India; E-mails: v.arch17@gmail.com, mangu167@yahoo.co.in, akpandey23@rediffmail.com

reported for the first time the microbiocidal effect of the platinised TiO<sub>2</sub>. Since then research work on antibacterial effects of TiO<sub>2</sub> has been intensively conducted against a wide spectrum of pathogenic microorganisms including bacteria, viruses, fungi and algae [25-32].

Biological impacts of commercially available nanoscale titanium dioxide (TiO<sub>2</sub>) have been conducted by many researchers [33-43]. But, since TiO<sub>2</sub> is highly successful, commercialized and non-toxic, there is an interest in improving the activity of TiO<sub>2</sub> for antibacterial application. However, two barriers limit the use of TiO<sub>2</sub> for photocatalytic inactivation of bacteria: its relatively low efficiency of light utilization due to its wide band gap (3.0-3.2 eV) and its poor charge transfer properties. One such approach is to shift the band onset from UV into the visible region of the spectrum as 98% of photons from solar energy have wavelengths > 385 nm. The vast increase in number of available photons into the visible region should also improve the photocatalytic properties.

*Bauhinia variegata* (*B. variegata*) and *Tinospora cordifolia* (*T. cordifolia*) are medicinal plants traditionally used for various purposes. Here, in this effort we report for the first time an approach to enhance the antibacterial activities of TiO<sub>2</sub> by direct synthesizing plant extracts/TiO<sub>2</sub> composite *via* in-situ sol-gel polymerization method. The antibacterial activity of pure TiO<sub>2</sub>, plant extracts of *B. variegata* and *T. cordifolia*, and plant extracts/TiO<sub>2</sub> nanocomposite was tested and compared against two microorganisms' namely *E. faecalis* and *E. coli*. Our experimental results clearly reveal an enhanced antibacterial activity of plant extracts/TiO<sub>2</sub> nanocomposite compared to that of pure TiO<sub>2</sub> and pure plant extracts. In addition, we have seen many reports on antibacterial activity of TiO<sub>2</sub> against *E. coli* but no report on antibacterial activity of TiO<sub>2</sub> against *E. faecalis*. So, this is also the first report on antibacterial activity of TiO<sub>2</sub> against microorganism *E. faecalis*.

## 2. EXPERIMENTAL DETAILS

### 2.1. Plant Material

The leaves of plants *B. variegata* and stem of *T. cordifolia* were collected from Botanical garden, University of Allahabad, Allahabad, India. Freshly collected plant parts were shade-dried at room temperature for 10-15 days. The samples were separately crushed into fine powder with mortar and pestle.

### 2.2. Extraction of Plant Materials

Various organic solvents were used for the extraction of bioactive compounds. The solvent used for extraction included petroleum ether (PE), benzene (BZ), chloroform (CH), ethyl acetate (EA), acetone (AC), ethanol (ET) and water (aqueous). Powdered plant materials were sequentially extracted with different solvents in a Soxhlet apparatus for 8 h according to the method described elsewhere [44]. The respective extracts were filtered and dried under reduced pressure using rotary evaporator to yield solid residues.

### 2.3. Preparation of Pure TiO<sub>2</sub>

For preparing pure TiO<sub>2</sub> we have used anhydrous titanium (IV) chloride (MERCK) and ethanol (MERCK). 30  $\mu$ L of titanium (IV) chloride (TiCl<sub>4</sub>) was dissolved in 20 ml of absolute ethanol under constant magnetic stirring. The entire process was carried out at room temperature. The solution gradually turned into transparent soft gel. The solution was further stirred for another half an hour under UV radiation (20 W, with a light intensity of approximately 1 mW cm<sup>-2</sup>) in order to sterilize the surface and then aged in static condition at room temperature. The soft gel continued to change with time, from translucent to milky white. The resulting precipitate was recovered by centrifugation process followed by washing several times with ethanol and then dried at temperature of 70°C. In order to get finally divided TiO<sub>2</sub> nanopowder the sample was crushed in mortar and pestle.

### 2.4. Preparation of Plant Extract/TiO<sub>2</sub> Composite

500 mg of prepared plant extract was dissolved in 20 ml of ethanol under magnetic stirring and after that 30  $\mu$ L of titanium (IV) chloride (TiCl<sub>4</sub>) was added in it. The process of stirring was continued for half an hour under UV radiation (20 W, with a light intensity of approximately 1 mW cm<sup>-2</sup>). Finally we get plant extract/TiO<sub>2</sub> composite residues. The composite residue was dried at temperature of 70°C and was crushed in mortar and pestle. The procedure was done for all the seven extracts of *B. variegata* and all the seven extracts of *T. cordifolia* separately to prepare plant extract/TiO<sub>2</sub> composite.

### 2.5. Microorganisms

Bacterial strain of *E. faecalis* (Gram-positive) and *E. coli* (Gram-negative) were obtained from Microbiology Department, MLN Medical College, Allahabad, India.

Microorganisms were streaked on nutrient agar plates and incubated at 37 °C for approximately 24 h to obtain isolated, actively growing colonies.

## 2.6. Antibacterial Activity Measurement

Antibacterial activity was demonstrated using a modification of the method originally described by Bauer *et al.* which is widely used for the antibacterial susceptibility testing [45]. The solid composite residue was dissolved in 1 ml of ethanol and 20 µL (containing 10 mg of plant extract and 0.5 mg of TiO<sub>2</sub> nanoparticles) of this dissolved residue was applied to sterile blank paper disk (6 mm diameter, 0.6 mm thick) using a pipette and disposable tip. Negative control disks were prepared with 20 µL of 95% ethanol. All the plant extracts/TiO<sub>2</sub> composites and negative controls were tested with triplicate disks. After applying the composites, the disks were immediately placed equidistantly on the surface of the Mueller-Hinton plates (100 × 15 mm) and lightly tamped down with a pair of sterile forceps. The plates were placed upright in a refrigerator at 5°C for 10-15 min to allow for maximum diffusion of the extracts. The plates were removed from the refrigerator and incubated inverted at 37 °C for 24 h. The diameters of the zones of inhibition (ZOI) were measured with a transparent ruler and recorded in millimeters, with estimates being made to the nearest 0.5 mm. The diameters of the zones of inhibition for the triplicate disks were averaged and rounded to the nearest millimeters. The same procedures have been made with the bulk TiO<sub>2</sub>, nano TiO<sub>2</sub> and pure plant extracts for comparative study.

## 2.7. Characterization Techniques

X'Pert Data with Cu-Kα line ( $\lambda = 1.54\text{\AA}$ ) was used for recording X-ray diffraction (XRD) pattern operating at 30kV and 30mA in the  $2\theta$  range 20° – 60°. Surface morphology of the as prepared samples was studied by a JEOL SET scanning electron microscopy with an accelerating voltage of 15.0 kV in a high vacuum mode to achieve magnification between 100× and 10,000×. The UV-visible spectra were recorded on Lambda 35 Perkin Elmer in the range 200-800 nm.

## 3. RESULTS AND DISCUSSION

The structural evolution of the pure TiO<sub>2</sub> and plant extract/TiO<sub>2</sub> composite was investigated by XRD. Figure 1 shows the XRD patterns of pure TiO<sub>2</sub> and plant extract/TiO<sub>2</sub> composites. The XRD results clearly confirm the presence of TiO<sub>2</sub> in the plant extract/TiO<sub>2</sub> composite sample. All the diffraction peaks of Figure 1a

could be indexed as tetragonal TiO<sub>2</sub> rutile structure (JCPDS file no. 21-1276). It is well known that an increase in full width at half maximum (FWHM) value results a subsequent decrease in crystallite size. The peaks of TiO<sub>2</sub> are wide, which means grain size of TiO<sub>2</sub> is rather small. The average crystallite size 'd' in nanometer has been calculated making use of the Scherer formula i.e.  $d \text{ (nm)} = \frac{0.9\lambda}{B(2\theta)\cos\theta}$ , where  $\lambda$  is

the wavelength of the X-rays ( $\lambda = 1.5 \text{\AA}$ ),  $B(2\theta)$  is the full width at the half maximum intensity (FWHM) and  $\theta$  is the diffraction angle in degrees [46]. From the broadening of the X-ray diffraction peaks, the average crystallite size of pure TiO<sub>2</sub> is calculated to be in the range of ~ 3 to 8 nm. The XRD pattern of *T. cordifolia*/TiO<sub>2</sub> composite shows peak of rutile TiO<sub>2</sub> corresponding to planes (110) and (101). The average crystallite size for this composite sample comes out to be ~ 8 to 10 nm. In the XRD spectra of *B. variegata*/TiO<sub>2</sub> composite additional diffraction peak of titanium monoxide (TiO) also appears. The possible explanation for this can be given by assuming the formation of TiO molecules as a result of chemical reaction between Ti and TiO<sub>2</sub> under such experimental condition. The average crystallite size for *B. variegata*/TiO<sub>2</sub> composite sample is calculated in the range of ~ 6 to 20 nm.

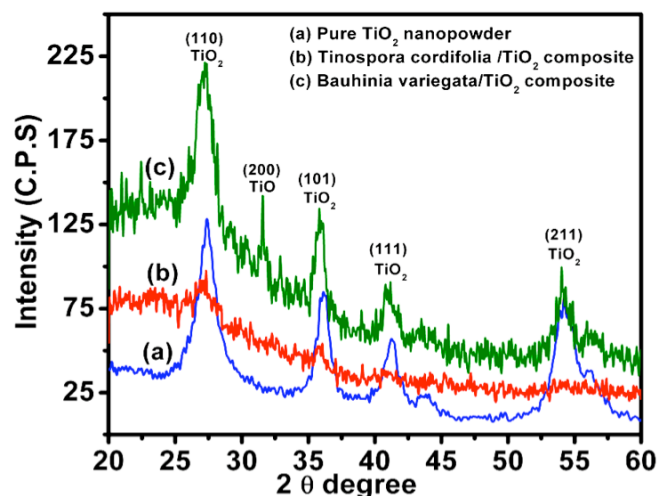


**Figure 1:** XRD patterns of (a) pure TiO<sub>2</sub>, (b) *T. cordifolia*/TiO<sub>2</sub> composite and (c) *B. variegata*/TiO<sub>2</sub> nanocomposite.

The surface morphology of pure TiO<sub>2</sub>, *B. variegata*/TiO<sub>2</sub> and *T. cordifolia*/TiO<sub>2</sub> composites are shown in Figure 2a, 2b and 2c respectively. The SEM images indicate the formation of irregularly shaped particles with some agglomeration. The uniformity of TiO<sub>2</sub> coated with plant extracts allows an estimation of the area of contact with the bacteria. The agglomeration of nanoparticles constitutes the micro-particles which may decrease the capability of nanoparticles to penetrate the cellular structure. So, no size related toxic effect is expected.

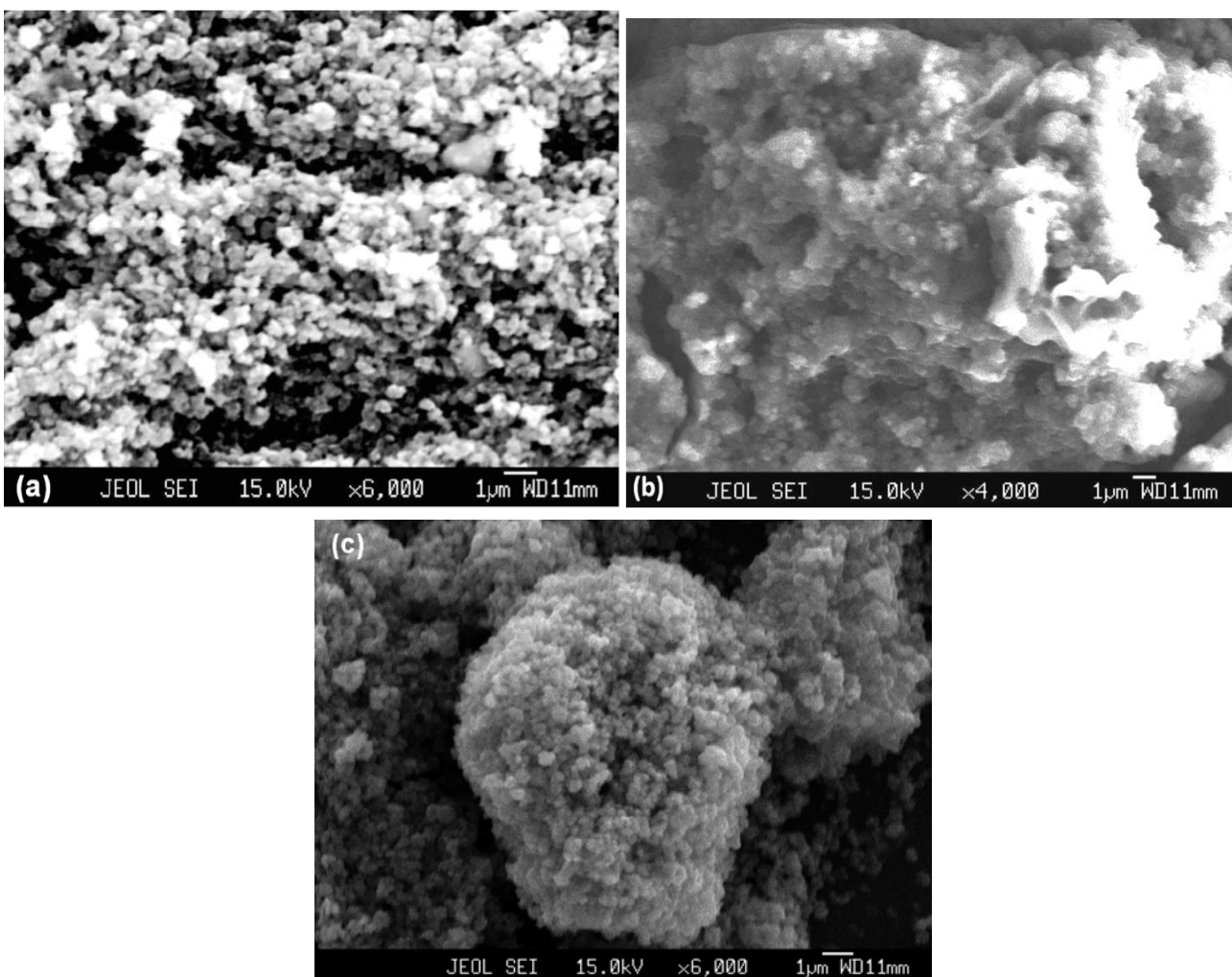


**Figure 2:** SEM photographs of agglomeration of nanoparticles (a) pure  $\text{TiO}_2$  (b) *B. variegata*/ $\text{TiO}_2$  composite and (c) *T. cordifolia*/ $\text{TiO}_2$  composite samples.

The UV-vis absorption spectra of  $\text{TiO}_2$ , *B. variegata* and *T. cordifolia* exhibited absorption at region below 400 nm, as shown in Figure 3. Figure 4 shows the UV-vis absorption spectra of  $\text{TiO}_2$ , *B. variegata*/ $\text{TiO}_2$  and *T. cordifolia*/ $\text{TiO}_2$  nanocomposites. Note that the absorption edges of both the plant extract/ $\text{TiO}_2$  nanocomposites are red-shifted from that of the  $\text{TiO}_2$  indicating that optical properties of  $\text{TiO}_2$  get functionalized in the presence of plant extracts. This also means that aqueous *B. variegata*/ $\text{TiO}_2$  and *T. cordifolia*/ $\text{TiO}_2$  nanocomposites would be candidate photocatalysis because there is a corresponding relation between the absorption intensity of UV radiation and the activity of photocatalyst [47]. The stronger the UV absorption intensity, the higher the activity, where the stronger absorption intensity implied that more electrons could be promoted from the valence band into the conduction band and more separate electrons or holes could be produced, which will help to enhance the photocatalytic activity.

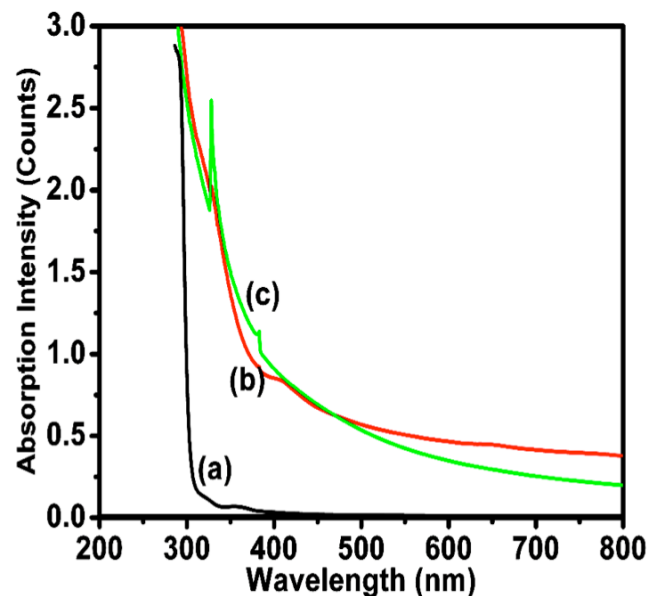


**Figure 3:** UV-vis absorption spectrum of (a) pure  $\text{TiO}_2$  (b) aqueous extract of *B. variegata* and (c) aqueous extract of *T. cordifolia* samples.

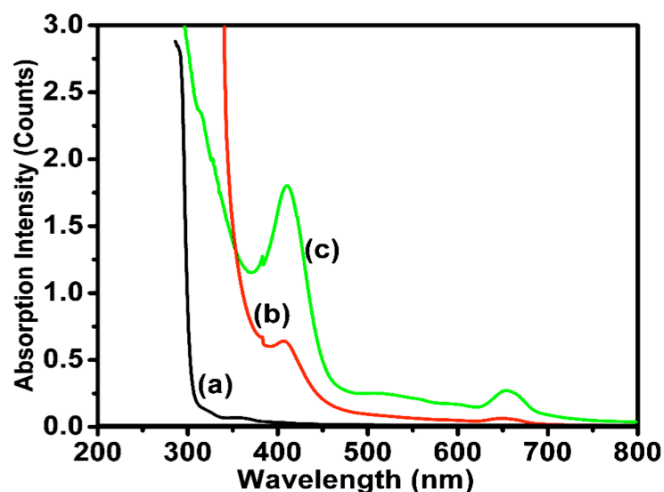


**Figure 4:** UV-vis absorption spectrum of (a) pure TiO<sub>2</sub> (b) aqueous extract of *B. variegata*/TiO<sub>2</sub> composite and (c) aqueous extract of *T. cordifolia*/TiO<sub>2</sub> nanocomposite samples.

The antibacterial activities of the samples were evaluated by the inactivation of *E. faecalis* (Gram positive) and *E. coli* (Gram negative), on the basis of the zone of inhibition (ZOI) surrounding disks on agar plates. The antibacterial activities of the pure extracts

of *B. variegata* and *T. cordifolia* are shown in Table 1. As can be seen from the Table 1, only ethanol, benzene and petroleum ether extracts of pure *B. variegata* showed antibacterial activity against *E. faecalis* (ZOI, 9-10 mm). However, for *E. coli*, all the extracts of *B. variegata* except acetone and ethanol have shown the antibacterial activity (ZOI, 8-11 mm). On the other hand *T. cordifolia* extracts showed various antibacterial activities (9-15 mm) against *E. faecalis* and all the extracts except acetone and benzene have shown antibacterial activity of 7-13 mm against *E. coli*.

The inactivation behavior of the two microorganisms against prepared plant extract/TiO<sub>2</sub> nanocomposites is shown in Table 2. Graphs representing a comparative inactivation behavior of *E. faecalis* and *E. coli* by pure plant extract and that of plant extract/TiO<sub>2</sub> nanocomposites are shown in Figures 5 and 6, respectively. In the control test, for bulk TiO<sub>2</sub> (MERK, purchased) and pure alcohol, no inactivation of the both microorganisms was observed which proves that bulk TiO<sub>2</sub> and alcohol could not act as antibacterial agents. However, pure TiO<sub>2</sub> nanoparticles showed ZOI

**Table 1: Mean Diameter of Inhibitory Zone (mm) Exhibited by Pure Plant Extracts of *Bauhinia variegata* and *Tinospora cordifolia* Against Bacterial Strains *Enterococcus faecalis* and *Escherichia coli***

Extracts	<i>Enterococcus faecalis</i>		<i>Escherichia coli</i>	
	<i>Bauhinia Variegata</i>	<i>Tinospora cordifolia</i>	<i>Bauhinia Variegata</i>	<i>Tinospora cordifolia</i>
Petroleum Ether	10 mm	11 mm	09 mm	13 mm
Benzene	09 mm	13 mm	08 mm	×
Chloroform	×	11 mm	09 mm	10 mm
Ethyl Acetate	×	12 mm	11 mm	07 mm
Acetone	×	15 mm	×	×
Ethanol	10 mm	10 mm	×	09 mm
Aqueous	×	09 mm	08 mm	08 mm

**Table 2: Mean Diameter of Inhibitory Zone (mm) Exhibited by Composite Plant Extracts of *Bauhinia variegata*/TiO<sub>2</sub> and *Tinospora cordifolia*/TiO<sub>2</sub> Against Bacterial Strains *Enterococcus faecalis* and *Escherichia coli***

Extracts	<i>Enterococcus faecalis</i>		<i>Escherichia coli</i>	
	<i>Bauhinia variegata</i> /TiO <sub>2</sub>	<i>Tinospora cordifolia</i> /TiO <sub>2</sub>	<i>Bauhinia variegata</i> /TiO <sub>2</sub>	<i>Tinospora cordifolia</i> /TiO <sub>2</sub>
Petroleum Ether	×	22 mm	15 mm	15 mm
Benzene	×	26 mm	09 mm	×
Chloroform	15 mm	×	12 mm	17 mm
Ethyl Acetate	14 mm	×	12 mm	×
Acetone	×	×	12 mm	×
Ethanol	×	×	13 mm	13 mm
Aqueous	45 mm	14 mm	30 mm	×

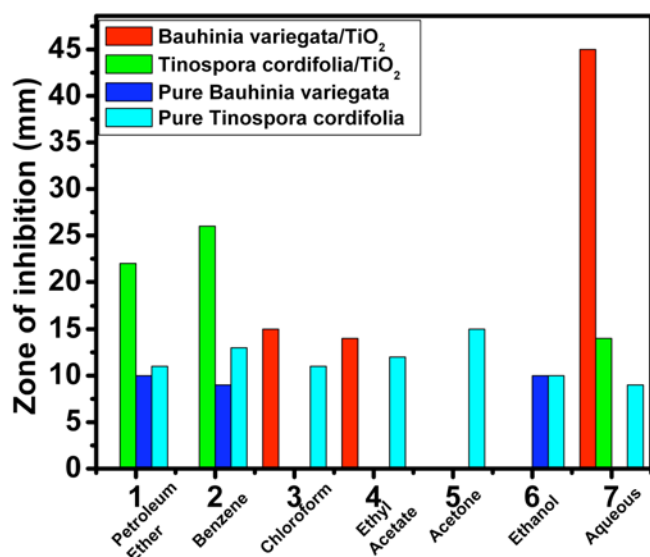


**Figure 5:** Graph showing inactivation of *E. faecalis* by pure plant extracts and that of plant extract/TiO<sub>2</sub> nanocomposites.

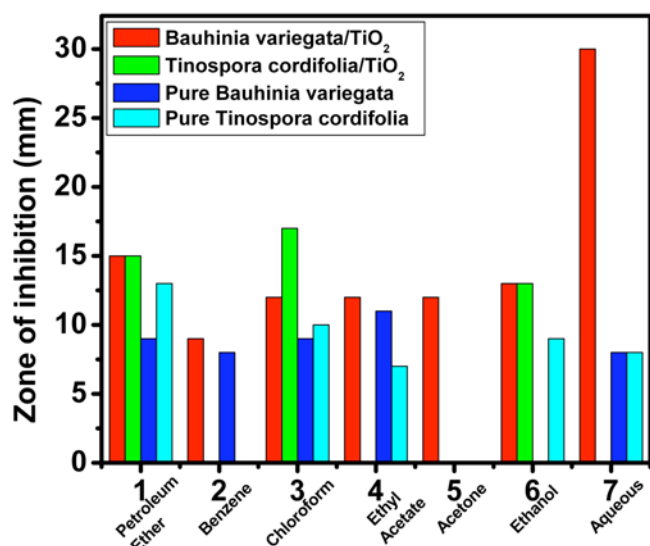


**Figure 6:** Graph showing inactivation of *E. coli* by pure plant extracts and that of plant extract/TiO<sub>2</sub> nanocomposites.

of 20 mm against *E. faecalis* and 14 mm against *E. coli*. Table 2 indicates that Gram negative bacteria *E. coli* were inhibited by all the samples of *B. variegata*/TiO<sub>2</sub> composite. However, the highest antibacterial activity was observed in aqueous extract of *B. variegata*/TiO<sub>2</sub> nanocomposite showing ZOI of 30 mm against *E. coli* (see Figure 7b). For *T. cordifolia*/TiO<sub>2</sub> nanocomposites only extracts in ethanol, chloroform and petroleum ether exhibited inhibition against *E. coli* (13-17 mm). For *E. faecalis*, out of seven samples of *B. variegata*/TiO<sub>2</sub> nanocomposite, only three extracts namely chloroform, ethyl acetate and aqueous were found to be active. In this case also the highest activity was exhibited by aqueous extract of *B. variegata*/TiO<sub>2</sub> nanocomposite

showing ZOI of 45 mm (see Figure 7a). For *T. cordifolia*/TiO<sub>2</sub> nanocomposite sample only extracts of petroleum ether, benzene and aqueous showed inhibition against *E. faecalis* (14-26 mm). Such kinds of antibacterial activity against *E. faecalis* and *E. coli* have not been reported previously by either TiO<sub>2</sub> or by any other biologically active material to the best of our knowledge. The highest antibacterial activity exhibited by aqueous extract of *B. variegata*/TiO<sub>2</sub> nanocomposite may be due to the presence and association of reactive oxygen species (ROS) generated by TiO<sub>2</sub> photocatalytic reactions that are directly involved in the oxidation process leading to the degradation of microorganisms [48-54], and to improved attraction and surface hydrophilic properties. Furthermore, the modification of surface charges due to the formation of titanium monoxide (TiO) in the plant extract/TiO<sub>2</sub> nanocomposite should also be taken into account. Generation of ROS causes oxidative damages to living organism suggesting that the cell membrane is the primary site of ROS attack. The cell membrane damage directly leads to the leakage of minerals, proteins, and genetic materials which is the root cause of cell death [55]. Some plant extract/TiO<sub>2</sub> nanocomposites exhibited no/lower antibacterial activity against tested bacterial strains which may be due to some kind of resistance mechanism of bacterial strain e.g. enzymatic inactivation, target sites modification and decreased intracellular drug accumulation towards these nanocomposites [56] or due to nature of solvents modifying the properties of nanocomposite. Comparatively better inhibitory efficacy of nanocomposites was observed against *E. faecalis* (Gram-positive). It could be substantiated by the reports that Gram-negative bacteria are more resistant to plant extracts than Gram-positive bacteria. Such resistance could be due to the permeability barrier provided by the cell wall or to the membrane accumulation mechanism [44]. Thus we observed that depending on the synthesis methodology adopted for testing antibacterial activity, the most diverse results can be obtained. It is therefore recommended that tested plant extract/TiO<sub>2</sub> composite could be used as novel medicine for treatment of bacterial infections, especially for antibiotic resistant bacterial infections.

#### 4. CONCLUSIONS

The study demonstrates a novel approach to use TiO<sub>2</sub> for antibacterial purpose in composite form with plant extract. XRD investigations have confirmed the presence of TiO<sub>2</sub> in the prepared plant extract/TiO<sub>2</sub> composite samples. UV-vis measurements revealed an

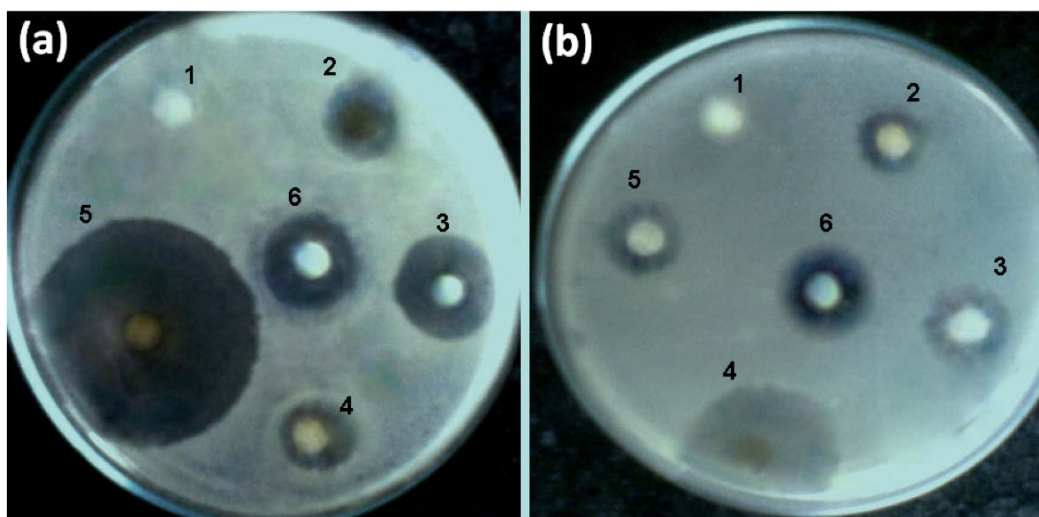


**Figure 7:** Discs representing ZOI from *B. variegata*/TiO<sub>2</sub> and *T. cordifolia*/TiO<sub>2</sub> nanocomposite in case of (a) *E. faecalis*: (1) control-ET (2) B.v.-CH/TiO<sub>2</sub> (3) T.c.-BZ/TiO<sub>2</sub> (4) B.v.-EA/TiO<sub>2</sub> (5) B.v.-AQ/TiO<sub>2</sub> (6) T.c.-PE/TiO<sub>2</sub>; and (b) *E. coli*: (1) control-ET (2) T.c.-ET/TiO<sub>2</sub> (3) T.c.-CH/TiO<sub>2</sub> (4) B.v.-AQ/TiO<sub>2</sub> (5) T.c.-PE/TiO<sub>2</sub> (6) B.v.-PE/TiO<sub>2</sub>. Where PE- petroleum ether, BZ-benzene, CH-chloroform, EA-ethyl acetate, AC-acetone, ET-ethanol and AQ-water. B.v.- *B. variegata* and T.c.- *T. cordifolia*.

enhanced absorption capability and hence an enhanced photocatalytic activity of plant extract/TiO<sub>2</sub> composites. The plant extract/TiO<sub>2</sub> composite showed tremendously improved antibacterial activity against *E. faecalis* and *E. coli* which have not been observed and reported previously to the best of our knowledge. However, there is no report on such kind of antibacterial activity of TiO<sub>2</sub> against the microorganism *E. faecalis* which we have observed in our case. Since the approach seemed to be very effective, further research is necessary for successful synthesis and characterization of these types of biologically active composite/ composites containing TiO<sub>2</sub> in the field of nanomedicines, especially for antibacterial purpose.

## ACKNOWLEDGEMENTS

The authors would like to acknowledge "National Center of Experimental Mineralogy and Petrology" for providing XRD and SEM experimental facilities. Prof. Ram Gopal is also acknowledged for providing UV-Vis spectroscopy facility.

## REFERENCES

- [1] Fisher K, Phillips C. The ecology, epidemiology and virulence of Enterococcus. *Microbiology* 2009; 155(Pt 6): 1749-57. <http://dx.doi.org/10.1099/mic.0.026385-0>
- [2] Ryan KJ, Ray CG, Ed. *Sherris Medical Microbiology* (4<sup>th</sup> ed.), McGraw Hill, 2004; pp. 294-295. ISBN 0-8385-8529-9.
- [3] Willett HP. Energy metabolism. In: Joklik WK, Willett HP, Amos DB, Wilfert CM, Eds. *Zinsser microbiology*. 20<sup>th</sup> ed. East Norwalk (CT): Appleton & Lange 1992; pp. 53-75.
- [4] Manning SAI, Heymann D, *Escherichia Coli Infections* (Deadly Diseases and Epidemics). Chelsea House Publications: New York 2004.
- [5] Cho M, Kim J, Kim JY, Yoon J, Kim JH. Mechanisms of *Escherichia coli* inactivation by several disinfectants. *Water Res* 2010; 44(11): 3410-8. <http://dx.doi.org/10.1016/j.watres.2010.03.017>
- [6] Boettcher H. Bioactive sol-gel coatings. *J Prakt Chem* 2000; 342: 427-36. <http://dx.doi.org/10.1002/chin.200040296>
- [7] Couto DS, Alves NM, Mano JF. Nanostructured multilayer coatings combining chitosan with bioactive glass nanoparticles. *J Nanosci Nanotechnol* 2008; 8: 1-8.
- [8] Chan G, Mooney DJ, New materials for tissue engineering: towards greater control over the biological response. *Trends Biotechnol* 2008; 26: 382-92. <http://dx.doi.org/10.1016/j.tibtech.2008.03.011>
- [9] Khan SUM, Al-Shahry M, Ingler WB Jr. Efficient Photochemical Water Splitting by a Chemically Modified n-TiO<sub>2</sub>. *Science* 2002; 297: 2243-45. <http://dx.doi.org/10.1126/science.1075035>
- [10] Hou K, Tian BZ, Li FY, Bian ZQ, Zhao DY, Huang CH. Highly crystallized mesoporous TiO<sub>2</sub> films and their applications in dye sensitized solar cells. *J Mater Chem* 2005; 15: 2414-20. <http://dx.doi.org/10.1039/b417465h>
- [11] Liu S, Chen A. Coadsorption of Horseradish Peroxidase with Thionine on TiO<sub>2</sub> Nanotubes for Biosensing. *Langmuir* 2005; 21: 8409-13. <http://dx.doi.org/10.1021/la050875x>
- [12] Topoglidis E, Cass AEG, Gilardi G, Sadeghi S, Beaumont N, Durrant JR. Protein Adsorption on Nanocrystalline TiO<sub>2</sub> Films: An Immobilization Strategy for Bioanalytical Devices. *Anal Chem* 1998; 70: 5111-13. <http://dx.doi.org/10.1021/ac980764j>
- [13] McKenzie KJ, Marken F. Accumulation and Reactivity of the Redox Protein Cytochrome c in Mesoporous Films of TiO<sub>2</sub> Phytate. *Langmuir* 2003; 19: 4327-31. <http://dx.doi.org/10.1021/la0267903>
- [14] Caballero L, Whitehead KA, Allen NS, Verran J. Photoinactivation of *Escherichia coli* on acrylic paint formulations using fluorescent light. *Dyes Pigments* 2010; 86: 56-62. <http://dx.doi.org/10.1016/j.dyepig.2009.12.001>
- [15] Labille J, Feng J, Botta C, et al. Aging of TiO<sub>2</sub> nanocomposites used in sunscreen. Dispersion and fate of

- the degradation products in aqueous environment. *Environ Pollut* 2010; 158: 3482-89.  
<http://dx.doi.org/10.1016/j.envpol.2010.02.012>
- [16] Zhu X, Wang J, Zhang X, Chang Y, Chen Y. Trophic transfer of TiO<sub>2</sub> nanoparticles from daphnia to zebrafish in a simplified freshwater food chain. *Chemosphere* 2010; 79: 928-33.  
<http://dx.doi.org/10.1016/j.chemosphere.2010.03.022>
- [17] Zhu X, Chang Y, Chen Y. Toxicity and bioaccumulation of TiO<sub>2</sub> nanoparticle aggregates in *Daphnia magna*. *Chemosphere* 2010; 78: 209-15.  
<http://dx.doi.org/10.1016/j.chemosphere.2009.11.013>
- [18] Gonçalves DM, Chiasson S, Girard D. Activation of human neutrophils by titanium dioxide (TiO<sub>2</sub>) nanoparticles. *Toxicol In Vitro* 2010; 24: 1002-1008.  
<http://dx.doi.org/10.1016/j.tiv.2009.12.007>
- [19] Zhu R-R, Wang W-R, Sun X-Y, Liu H, Wang S-L. Enzyme activity inhibition and secondary structure disruption of nano-TiO<sub>2</sub> on pepsin. *Toxicol In Vitro* 2010; 24: 1639-47.  
<http://dx.doi.org/10.1016/j.tiv.2010.06.002>
- [20] Demetrescu I, Pirvu C, Mitran V. Effect of nano-topographical features of Ti/TiO<sub>2</sub> electrode surface on cell response and electrochemical stability in artificial saliva. *Bioelectrochemistry* 2010; 79: 122-29.  
<http://dx.doi.org/10.1016/j.bioelechem.2010.02.001>
- [21] Sunada K, Watanabe T, Hashimoto K. Bactericidal Activity of Copper-Deposited TiO<sub>2</sub> Thin Film under Weak UV Light Illumination. *Environ Sci Technol* 2003; 37(20): 4785-89.  
<http://dx.doi.org/10.1021/es034106g>
- [22] Lin H, Xu Z, Wang X, et al. Photocatalytic and antibacterial properties of medical-grade PVC material coated with TiO<sub>2</sub> film. *J Biomed Mater Res B Appl Biomater* 2008; 87(2): 425-31.  
<http://dx.doi.org/10.1002/jbm.b.31120>
- [23] Linkous AC, Carter GJ, Locuson DB, Ouellette AJ, Slattery D, Simitha LA. Photocatalytic Inhibition of Algae Growth Using TiO<sub>2</sub>, WO<sub>3</sub>, and Cocatalyst Modifications. *Environ Sci Technol* 2000; 34(22): 4754.  
<http://dx.doi.org/10.1021/es001080+>
- [24] Matsunaga T, Tomoda R, Nakajima T, Wake H. Photoelectrochemical sterilization of microbial cells by semiconductor powders. *FEMS Microbiol Lett* 1985; 29: 211-16.  
<http://dx.doi.org/10.1111/j.1574-6968.1985.tb00864.x>
- [25] Kim DS, Kwak SY. Photocatalytic Inactivation of *E. coli* with a Mesoporous TiO<sub>2</sub> Coated Film Using the Film Adhesion Method. *Environ Sci Technol* 2009; 43: 148-51.  
<http://dx.doi.org/10.1021/es801029h>
- [26] Egerton TA, Kosa SAM, Christensen PA. Photoelectrocatalytic disinfection of *E. coli* suspensions by iron doped TiO<sub>2</sub>. *Phys Chem Chem Phys* 2006; 8: 398-406.  
<http://dx.doi.org/10.1039/b507516e>
- [27] Caballero L, Whitehead KA, Allen NS, Verran J. Inactivation of *Escherichia coli* on immobilized TiO<sub>2</sub> using fluorescent light. *J Photochem Photobiol A: Chem* 2009; 202: 92-98.  
<http://dx.doi.org/10.1016/j.jphotochem.2008.11.005>
- [28] Armelon L, et al. Photocatalytic and antibacterial activity of TiO<sub>2</sub> and Au/TiO<sub>2</sub> nanosystems. *Nanotechnology* 2007; 18: 375709.  
<http://dx.doi.org/10.1088/0957-4484/18/37/375709>
- [29] Maneerat C, Hayata Y. Antifungal activity of TiO<sub>2</sub> photocatalysis against *Penicillium expansum* *in vitro* and in fruit test. *Int J Food Microbiol* 2006; 107: 99-103.  
<http://dx.doi.org/10.1016/j.ijfoodmicro.2005.08.018>
- [30] Kangwansupamonkon W, et al. Antibacterial effect of apatite-coated titanium dioxide for textiles applications. *Nanomed Nanotechnol Biol Med* 2009; 5: 240-49.  
<http://dx.doi.org/10.1016/j.nano.2008.09.004>
- [31] Wu B, Huang R, et al. Bacterial responses to Cu-doped TiO<sub>2</sub> nanoparticles. *Sci Total Environ* 2010; 408: 1755-58.  
<http://dx.doi.org/10.1016/j.scitotenv.2009.11.004>
- [32] Su W, Wang S, Wang X, Fu X, Weng J. Plasma pre-treatment and TiO<sub>2</sub> coating of PMMA for the improvement of antibacterial properties. *Surface Coatings Technol* 2010; 205: 465-69.  
<http://dx.doi.org/10.1016/j.surfcoat.2010.07.013>
- [33] Jańczyk A, Wolnicka-Glubisz A, Urbanska K, Kisch H, Stochel G, Macyk W. Photodynamic activity of platinum(IV) chloride surface-modified TiO<sub>2</sub> irradiated with visible light. *Free Radical Biol Med* 2008; 44: 1120-30.  
<http://dx.doi.org/10.1016/j.freeradbiomed.2007.12.019>
- [34] Kangwansupamonkon W, Lauruengtana V, Surasmo S, Ruktanonchai U. Antibacterial effect of apatite-coated titanium dioxide for textiles applications. *Nanomed Nanotechnol Biol Med* 2009; 5: 240-49.  
<http://dx.doi.org/10.1016/j.nano.2008.09.004>
- [35] Cushnie TPT, Robertson PKJ, Ofcer S, Pollard PM, McCullagh C, Robertson JMC. Variables to be considered when assessing the photocatalytic destruction of bacterial pathogens. *Chemosphere* 2009; 74: 1374-78.  
<http://dx.doi.org/10.1016/j.chemosphere.2008.11.012>
- [36] Xekoukoulotakis NP, Xinidis N, Chroni M, et al. UV-A/TiO<sub>2</sub> photocatalytic decomposition of erythromycin in water: Factors affecting mineralization and antibiotic activity. *Catal Today* 2010; 151: 29-33.  
<http://dx.doi.org/10.1016/j.cattod.2010.01.040>
- [37] Ortega-Lara W, Cortés-Hernández DA, Best S, Brooks R, Hernández-Ramírez A. Antibacterial properties, *in vitro* bioactivity and cell proliferation of titania-wollastonite composites. *Ceram Int* 2010; 36: 513-19.  
<http://dx.doi.org/10.1016/j.ceramint.2009.09.024>
- [38] Hu CW, Li M, Cui YB, Li DS, Chen J, Yang LY. Toxicological effects of TiO<sub>2</sub> and ZnO nanoparticles in soil on earthworm *Eisenia fetida*. *Soil Biol Biochem* 2010; 42: 586-91.  
<http://dx.doi.org/10.1016/j.soilbio.2009.12.007>
- [39] Zhang HJ, Wen DZ. Antibacterial properties of Sb-TiO<sub>2</sub> thin films by RF magnetron co-sputtering. *Surface Coatings Technol* 2007; 201: 5720-23.  
<http://dx.doi.org/10.1016/j.surfcoat.2006.07.109>
- [40] Akhavan O. Lasting antibacterial activity of Ag-TiO<sub>2</sub>/Ag/a-TiO<sub>2</sub> nanocomposite thin film photocatalysts under solar irradiation. *J Colloidal Interf Sci* 2009; 336: 117-24.  
<http://dx.doi.org/10.1016/j.jcis.2009.03.018>
- [41] Skorb EV, Antonouskaya LI, Belyasova NA, Shchukin DG, Mohwald H, Sviridov DV. Antibacterial activity of thin-film photocatalysts based on metal-modified TiO<sub>2</sub> and TiO<sub>2</sub>:In<sub>2</sub>O<sub>3</sub> nanocomposite. *Appl Catal B: Environ* 2008; 84: 94-99.  
<http://dx.doi.org/10.1016/j.apcatb.2008.03.007>
- [42] Cheng Q, Li C, Pavlinek V, Saha P, Wang H. Surface-modified antibacterial TiO<sub>2</sub>/Ag<sup>+</sup> nanoparticles: Preparation and properties. *Appl Surface Sci* 2006; 252: 4154-60.  
<http://dx.doi.org/10.1016/j.apsusc.2005.06.022>
- [43] Dunnill CWH, Aiken ZA, Pratten J, Wilson M, Morgan DJ, Parkin IP. Enhanced photocatalytic activity under visible light in N-doped TiO<sub>2</sub> thin films produced by APCVD preparations using t-butylamine as a nitrogen source and their potential for antibacterial films. *J Photochem Photobiol A: Chem* 2009; 207: 244-53.  
<http://dx.doi.org/10.1016/j.jphotochem.2009.07.024>
- [44] Mishra AK, Mishra A, Bhargava A, Pandey AK. Antimicrobial activity of essential oils from the leaves of *Cinnamomum* spp. *Natl Acad Sci Lett* 2008; 31: 341-45.
- [45] Mishra A, Kumar S, Bhargava A, Sharma B, Pandey AK. Studies on *in vitro* antioxidant and antistaphylococcal activities of some important medicinal plants. *Cell Mol Biol* 2011; 57: 16-24.

- [46] Warren BE. X-Ray Diffraction (New York: Dover) 1990; p. 251.
- [47] Zhang Y, Xiong G, Yao N, Yang W, Fu X. Preparation of titania-based catalysts for formaldehyde photocatalytic oxidation from TiCl<sub>4</sub> by the sol-gel method. *Catal Today* 2001; 68: 89-95.  
[http://dx.doi.org/10.1016/S0920-5861\(01\)00295-4](http://dx.doi.org/10.1016/S0920-5861(01)00295-4)
- [48] Maness PC, Smolinski S, Blake DM, Huang Z, Wolfrum EJ, Jacoby WA. Bactericidal activity of photocatalytic TiO<sub>2</sub> reaction: toward an understanding of its killing mechanism. *Appl Environ Microbiol* 1999; 65: 4094-98.
- [49] Comparelli R, Fanizza E, Curri ML, *et al.* Photocatalytic degradation of azo dyes by organic-capped anatase TiO<sub>2</sub> nanocrystals immobilized onto substrates. *Appl Catal B* 2005; 55: 81-91.  
<http://dx.doi.org/10.1016/j.apcatb.2004.07.011>
- [50] Haick H, Paz Y. Remote Photocatalytic Activity as Probed by Measuring the Degradation of Self-Assembled Monolayers Anchored Near Micro-Domains of Titanium Dioxide. *J Phys Chem B* 2001; 105: 3045-51.  
<http://dx.doi.org/10.1021/jp0037807>
- [51] Wong M-S, Chu W-C, Sun D-S, *et al.* Visible-Light-Induced Bactericidal Activity of a Nitrogen-Doped Titanium Photocatalyst against Human Pathogens. *Appl Environ Microbiol* 2006; 72: 6111-16.  
<http://dx.doi.org/10.1128/AEM.02580-05>
- [52] Lu ZX, Zhou L, Zhang ZL, *et al.* Cell Damage Induced by Photocatalysis of TiO<sub>2</sub> Thin Films. *Langmuir* 2003; 19: 8765-68.  
<http://dx.doi.org/10.1021/la034807r>
- [53] Fu G, Vary PS, Lin C-T. Anatase TiO<sub>2</sub> Nanocomposites for Antimicrobial Coatings. *J Phys Chem B* 2005; 109(18): 8889-98.  
<http://dx.doi.org/10.1021/jp0502196>
- [54] Adams LK, Lyon DY, Alvarez PJJ. Comparative eco-toxicity of nanoscale TiO<sub>2</sub>, SiO<sub>2</sub>, and ZnO water suspensions. *Water Res* 2006; 40: 3527-32.  
<http://dx.doi.org/10.1016/j.watres.2006.08.004>
- [55] Schwarz S, Noble WC. Aspects of bacterial resistance to antimicrobials used in veterinary dermatological practice. *Veterin Dermatol* 1999; 10: 163-76.  
<http://dx.doi.org/10.1046/j.1365-3164.1999.00170.x>
- [56] Devasagayam TPA, Boloor KK, Ramsarma T. Methods for estimating lipid peroxidation: Analysis of merits and demerits (mini review). *Ind J Biochem Biophys* 2004; 40: 300-308.

Received on 25-08-2012

Accepted on 11-10-2012

Published on 31-10-2012

[DOI: http://dx.doi.org/10.6000/1929-5995.2012.01.01.6](http://dx.doi.org/10.6000/1929-5995.2012.01.01.6)